SLAC-PUB-2606
September 1980
(I)

PARTICLE IDENTIFICATION BY ČERENKOV AND TRANSITION RADIATION*

R. S. Gilmore

Stanford Linear Accelerator Center

Stanford University, Stanford, California 94305 USA

and

University of Bristol, H. H. Wills Physics Lab

Royal Fort, Tyndall Avenue, Bristol BS8 ITL, England

(Talk presented at the Proceedings of the Summer Institute on Particle Physics, Stanford, California, July 28 - August 8, 1980.)

*Work supported in part by the Department of Energy, under contract DE-AC03-76SF00515, and in part by the University of Bristol.

1. INTRODUCTION

Particle identification requires a measurement of the particle's mass and the sign of its electric charge, the particles of interest having unit charge. Passing the particle through a magnetic field gives the sign, from the direction of curvature of the track, and also a measure of the particle's momentum from the radius of curvature. The momentum, p, is given by

$$pc = m\beta\gamma \tag{1}$$

where

$$\beta = v/c$$

$$\gamma = \left(1 - \beta^2\right)^{-\frac{1}{2}}$$

so if the velocity, v, is measured; the mass is obtained. The precision with which the mass is determined is given by

$$\left(\frac{dm}{m}\right)^2 = \left(\gamma^2 \frac{d\beta}{\beta}\right)^2 + \left(\frac{dp}{p}\right)^2 \tag{2}$$

If the momentum p is relatively well measured, then the resolution of particles with masses m_1 and m_0 requires velocity resolution, $\Delta\beta$, given by

$$\frac{\Delta\beta}{\beta} = \frac{m_1^2 - m_0^2}{2p^2} \tag{3}$$

At low velocities, β may be measured by Time-of-Flight techniques, but at higher velocities Čerenkov counters are more suitable.

2. ČERENKOV RADIATION

A particle with electric charge e and velocity v in a medium of dielectric $\varepsilon(\omega)$ generates fields in the medium which, at large distances, b, may be expressed as in Equation (4) below[1]

$$\text{Parallel Electric Field} \qquad E_1(\omega) = \frac{ie\omega}{c^2}\left[1 - \frac{1}{\beta^2\varepsilon(\omega)}\right]\frac{e^{-\lambda b}}{\sqrt{\lambda b}}$$

$$\text{Transverse Electric Field} \qquad E_2(\omega) = \frac{e}{v\varepsilon(\omega)}\sqrt{\frac{\lambda}{b}}\; e^{-\lambda b} \tag{4}$$

$$\text{Transverse Magnetic Field} \qquad B_3(\omega) = \varepsilon(\omega)\beta E_2(\omega)$$

where

$$\lambda = \frac{\omega}{v}\sqrt{1 - \beta^2\varepsilon(\omega)}$$

At low speeds this gives fields which fall off exponentially away from the particle, the energy being carried along with the moving charge. However, if $\varepsilon(\omega)$ is real, i.e. there is no absorption, there will be some speed such that $\beta^2\varepsilon(\omega)$ is greater than unity (provided $\varepsilon(\omega) > 1$). In this case λ is imaginary and the fields take the form of a travelling wave. This corresponds to the case where the particle is travelling faster than the electromagnetic radiation in the medium. The energy in the field cannot return to the particle and is radiated as a shock wave in the direction $\underline{E} \times \underline{B}$, making an angle θ with the particle direction, where

$$\cos\theta = \frac{1}{\beta\sqrt{\varepsilon(\omega)}} = \frac{1}{\beta n(\omega)} \tag{5}$$

where $n(\omega)$ is the refractive index of the medium.

The energy spectrum of the radiation is given by

$$\left(\frac{dE}{d\omega}\right) = \frac{e^2}{c^2}\,\omega\left(1 - \frac{1}{\beta^2\left(\varepsilon(\omega)\right)}\right) \tag{6}$$

One is more interested in the number of photons, energy $\hbar\omega$, emitted from length L in energy range dE. This is

$$N = \frac{e^2}{\hbar^2 c^2} \sin^2\theta \, LdE \,, \qquad (7)$$

$$= 370 \sin^2\theta \, LdE \; ; \quad L \text{ in cm, } dE \text{ in eV}$$

The intensity of Čerenkov radiation in the visible region is low, typically one thirtieth of that from a scintillator of similar thickness. One of the main problems in Čerenkov counter design is the very low signal strength, often giving as little as three or four photoelectrons.

Though the intensity in the visible region is low, the Čerenkov spectrum extends far into the ultraviolet, the spectrum being approximately constant with respect to photon energy as long as the refractive index n is roughly constant and greater than $1/\beta$. Figure 1 shows that the refractive index of a typical radiator is roughly constant at low photon energy, has pronounced maxima and minima at the region's anomalous dispersion near atomic resonances, where strong absorption will inhibit radiation, and finally is less than unity for high photon energies. There is no Čerenkov radiation in the x-ray region as the refractive index is here less than unity.

For good particle identification you require dm/m to be low; hence, from Equation (2), you must determine $d\beta/\beta$ well. If you measure the Čerenkov angle θ, you get the greatest sensitivity when $d\theta/d\beta$ is large. Figure 2 is a plot of Čerenkov angle against β for various refractive indices and shows that $d\theta/d\beta$ is greatest near the threshold value of β. Near threshold, however, the value of θ is low, so the signal intensity is low. Alternatively, you can operate at larger values of θ and obtain

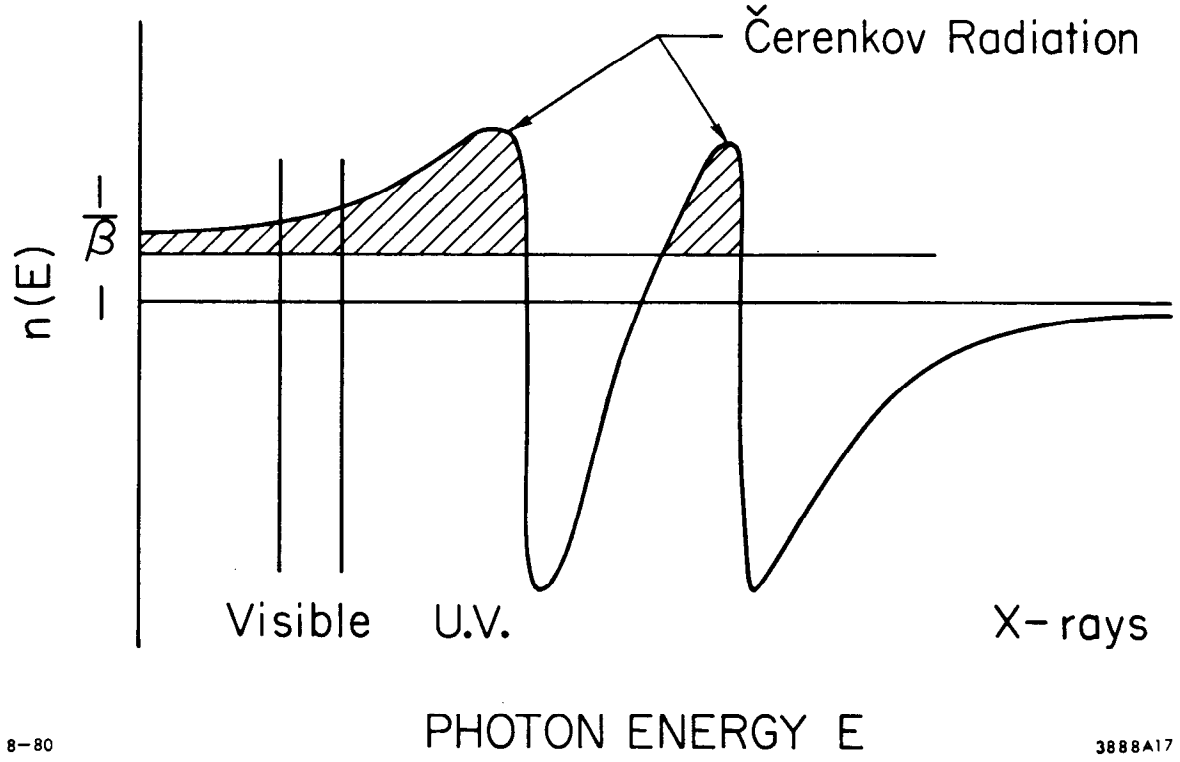

Fig. 1. Typical variation of refractive index with photon energy.

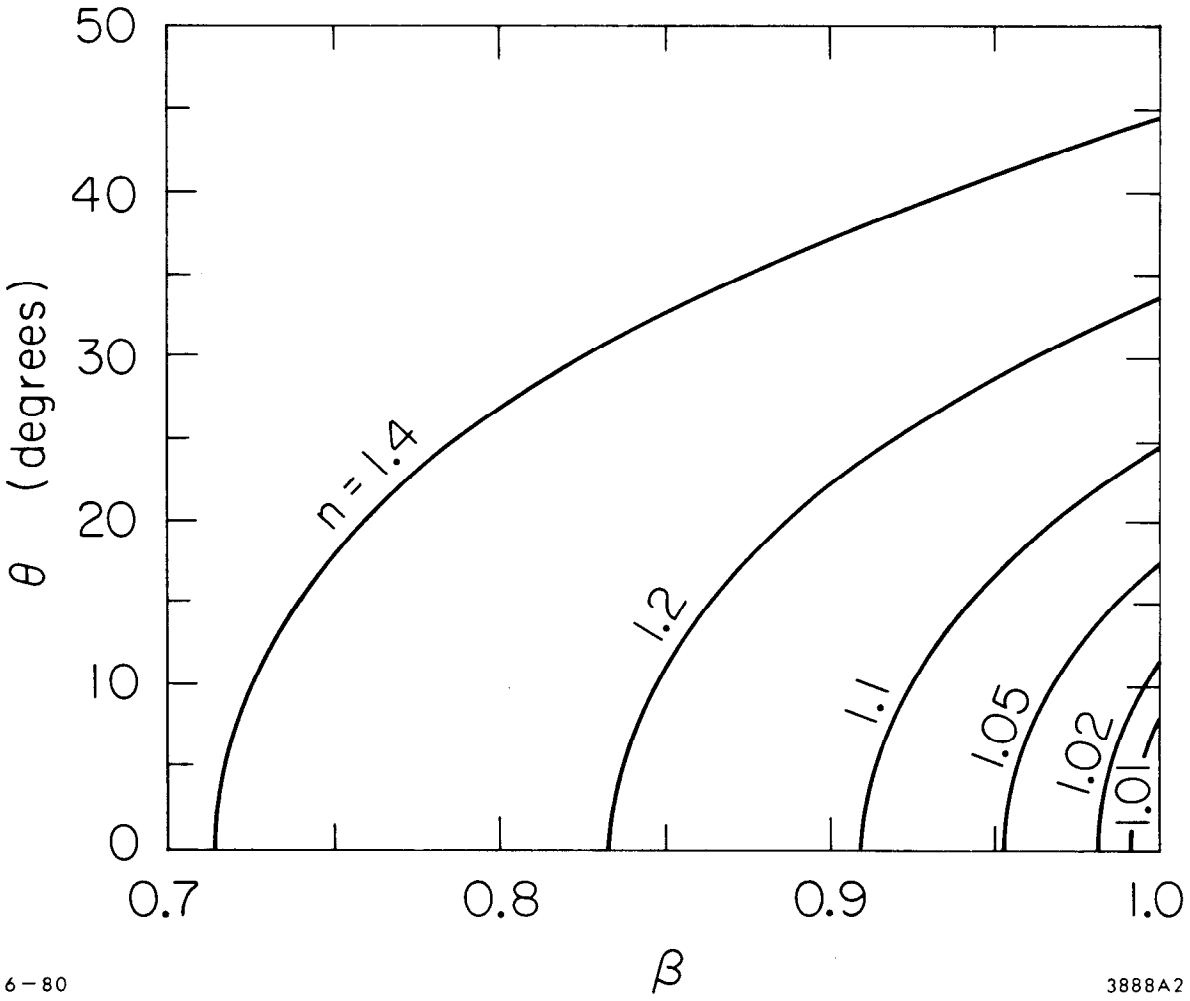

Fig. 2. Variation of Čerenkov angle θ with particle velocity β for several values of refractive index n.

more light, though $d\theta/d\beta$ will be lower. These possibilities correspond to the two main classes of Čerenkov counter, as shown in Figure 3. The threshold counter detects particles which emit light, and sees only those above the threshold velocity, while the differential counter selects particles giving light at a predetermined value of θ. Reference 2 gives an extensive review of both types of counter, with further references for conventional Čerenkov types.

3. THRESHOLD ČERENKOV

This detects a particle which produces enough light, in principle if $\beta > 1/n(\omega)$, but in practice β must be somewhat higher to give a signal large enough to be detected. It will detect any particle with higher β, e.g., a kaon detector will also detect pions and electrons of the same momentum.

The threshold counter has only one adjustable parameter, the refractive index of the radiator. To control the β threshold you must control the refractive index (e.g., vary the pressure in a gas filled counter). Figure 4 shows the appropriate refractive indices for pions and kaons of varying momentum. At very low momentum liquids and solids may be used, and at high momentum gasses either at atmospheric pressure or at pressures which are easy to obtain. It is difficult to obtain gas radiators in the refractive index range from 1.01 to 1.2 and here Aerogel counters are being used.[3] Aerogel is a mixture of air and small particles of silica, of typical size 10-100 nm. These are small relative to the wavelength of light observed and result in an effective refractive index between that of air and silica.

$n = 1 + 0.21\,\rho$ where ρ is the density in g/cm^3 .

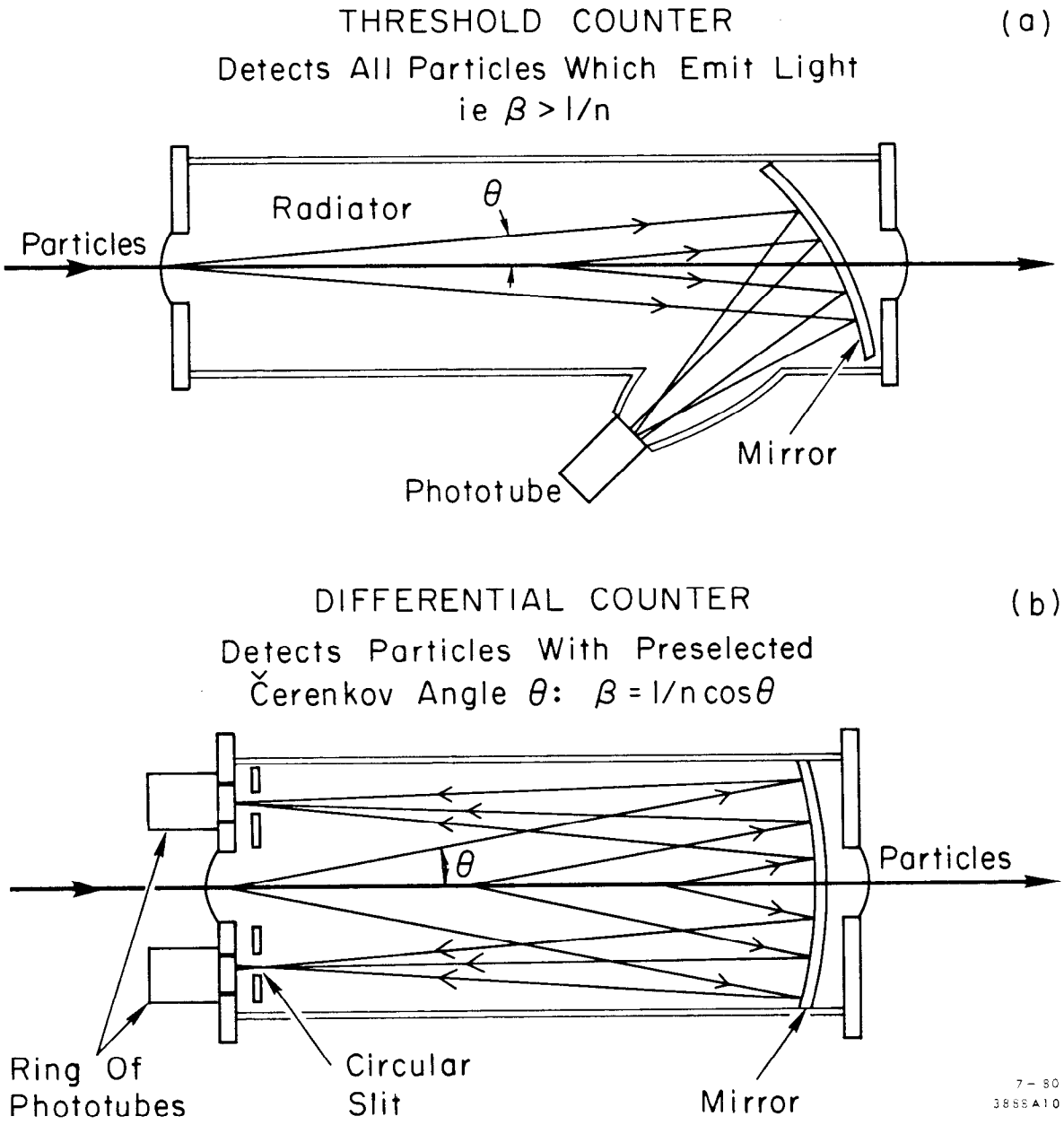

Fig. 3. The two principal classes of Čerenkov counter.

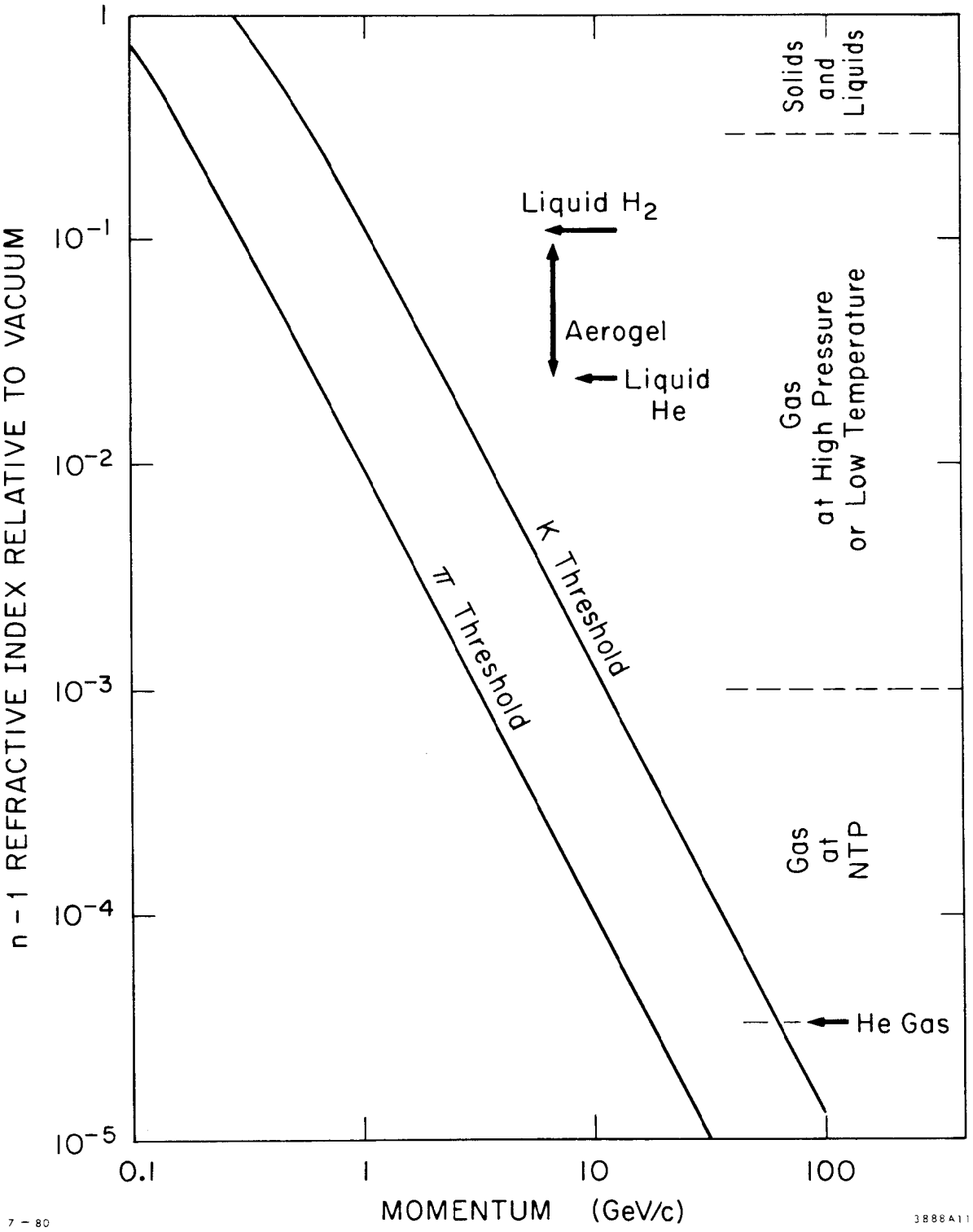

Fig. 4. The refractive index required so that of pions or kaons of given momentum be at threshold for Čerenkov radiation.

A pressure scan for a threshold counter[4] is shown in Figure 5. The detection efficiency for each type of particle arises gradually above threshold, showing that the resolution $\Delta\beta/\beta$ is limited. What effect limits the resolution? One contributing factor is the chromatic dispersion of the radiator medium, which will have a different refractive index for photons of different energy. The threshold β will vary with photon energy and give a spread, $\Delta\beta$, in resolution. For particles of different velocities β_1 and β_0 Equation (1) gives, for small values of θ,

$$\theta_1^2 - \theta_0^2 = 2(\beta_1 - \beta_2) = 2\Delta\beta \tag{8}$$

The spread in Čerenkov angles due to dispersion is

$$\Delta\theta_{DISP} = \frac{n-1}{n\nu \tan\theta} \tag{9}$$

where $\nu = (n-1)/\Delta n$ is the dispersive power of the medium.

The best signal is obtained for the detected particle by setting the slower particle exactly at threshold, where $\theta_0 = 0$ and it produces no light. Then you can show, using Equation (3), that

$$\frac{\Delta\theta_{DISP}}{\theta_1} \simeq \frac{1}{2\nu} \frac{m_1^2}{m_1^2 - m_0^2} \tag{10}$$

For counters operating in the visible region, this is usually small, of the order of a few percent for particles of interest, and it is not strongly dependent on momentum. Chromatic dispersion does not significantly limit the resolution of a threshold Čerenkov.

The slow rise in the efficiency of a Čerenkov counter is dominated by statistical fluctuations in the small number of photoelectrons produced. If n photons give nq detected photoelectrons, the probability

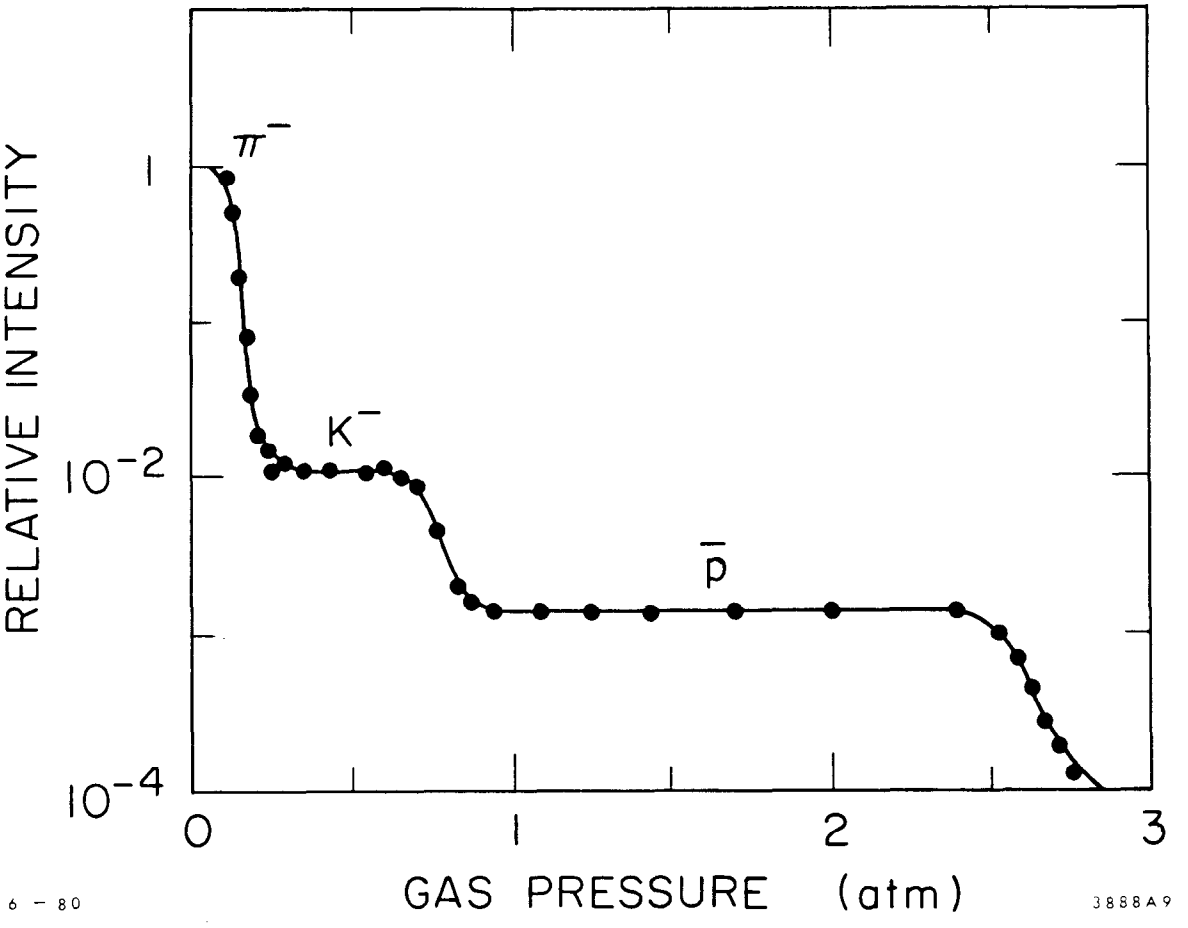

Fig. 5. Pressure scan for a five meter carbon dioxide filled threshold counter operating as a veto, for a beam of 20 GeV/c negative particles.

of detecting none is given by the Poisson expression e^{-nq}, so the efficiency is

$$\varepsilon = 1-e^{-nq} \quad . \tag{11}$$

Figure 6 shows how the efficiency varies with the number of photons detected.

As the number of photons emitted is proportional to $\sin^2\theta$, we see from Equation (8) that the number of photons is approximately proportional to $\Delta\beta$, for a threshold counter with the unwanted particle set at threshold. As the particle momentum, and hence γ, increases, the $d\beta/\beta$ required for particle separation decreases, from Equation (2), and hence the photon yield decreases. To maintain a reasonable efficiency you must take steps to recover an adequate number of photons. This may be attempted by

(a) Optimising the collection of light by the phototubes with a suitable choice of reflecting surfaces and geometry. This should be done in any Čerenkov counter but becomes more critical at high momentum.

(b) Increasing the length of the radiator. As the photon yield is proportional to radiator length this gives a direct improvement. Threshold counters for use at high momentum are many meters long.

(c) Increasing the range of photon energies detected. This again gives a proportional improvement, but is not easy to achieve. Phototubes with ultraviolet transmitting windows or ultraviolet converting phosphors can increase the range.[5]

Threshold counters have the advantage of relatively simple construction, all that is required is a large volume of radiator medium and an optical system to focus the light onto the detectors. Figure 7 shows a Čerenkov counter used in an experiment at CERN.[6] The only rigid section

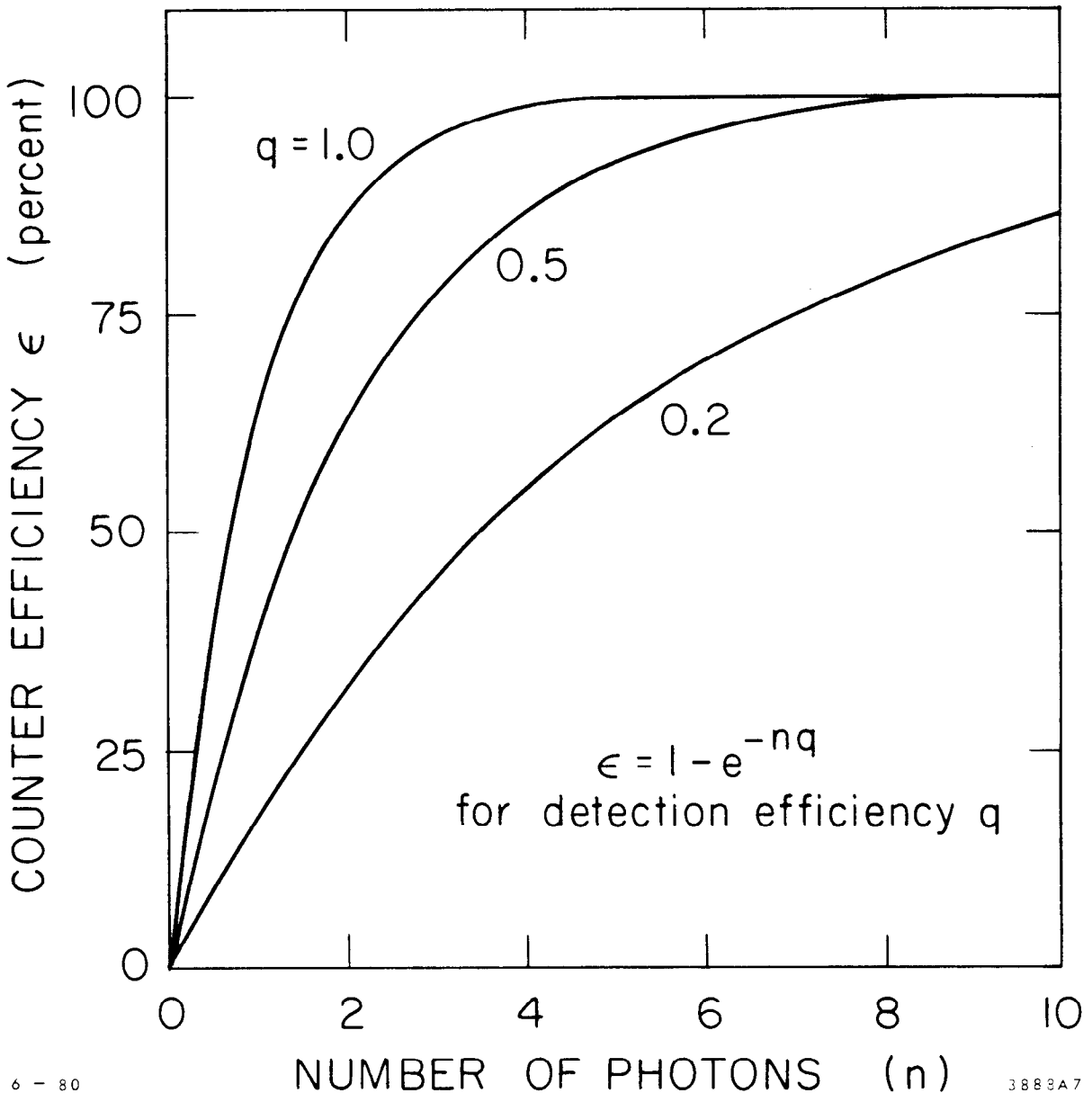

Fig. 6. Variation of the detection efficiency due to statistical fluctuations as a function of the number of photons.

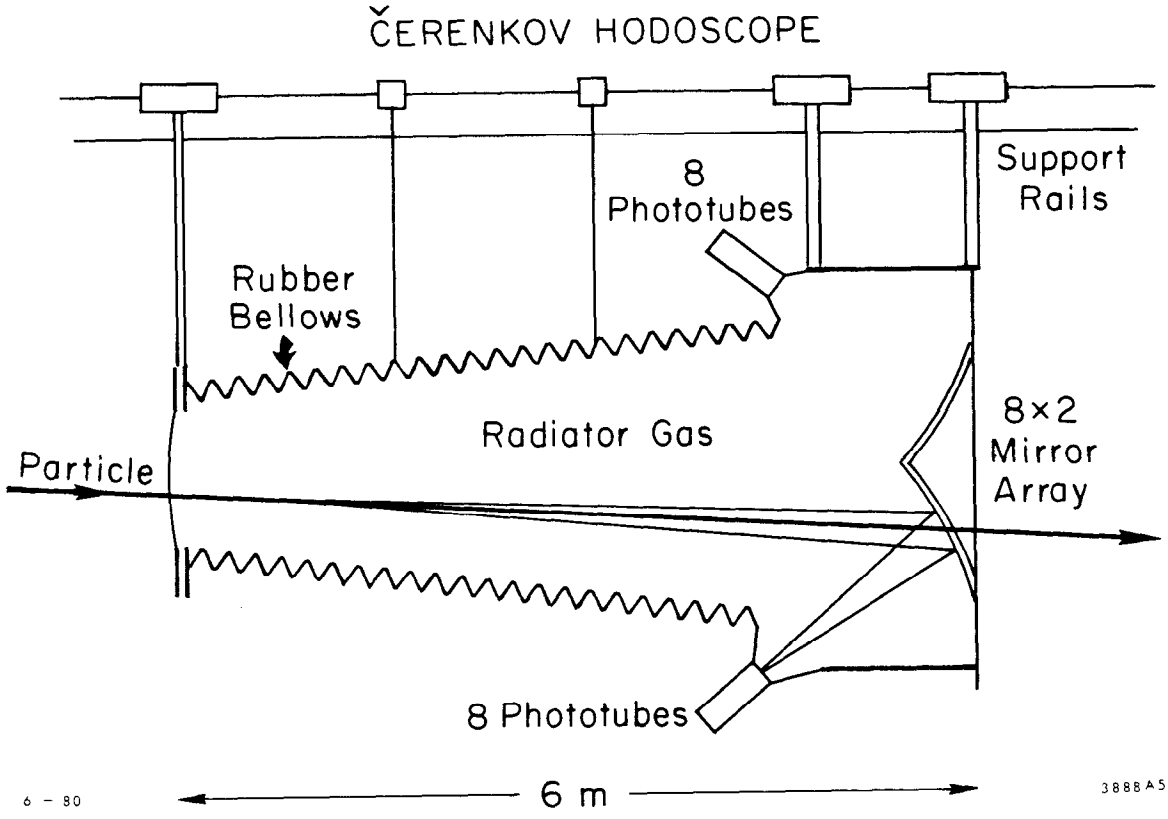

Fig. 7. Large modular threshold Čerenkov counter used in an experiment at CERN.

of this counter is the end box which holds the mirrors and phototubes. The main bulk of the counter is simply the radiator medium, and in this case is contained in a rubber bellows rather like an old camera, which can be folded up to allow access to other apparatus. The light collecting mirror is divided into sixteen sections, each of which is focused onto a different phototube. Such segmentation gives a threshold counter the ability to register several particles simultaneously, provided that they are sufficiently well separated that their Čerenkov light strikes different mirror sections.

4. DIFFERENTIAL ČERENKOV COUNTER

As Figure 3 shows, this uses a spherical mirror to produce a ring image for Čerenkov light at a given angle θ and detects the light corresponding to some angular range $\Delta\theta$ which passes through a circular diaphragm slit. This means that, unlike the threshold counter, for a given momentum p only one type of particle is detected.

The differential counter has two adjustable parameters — the refractive index, n, of the radiator and the detected Čerenkov angle θ. You can choose a larger Čerenkov angle for the detected particles than can be obtained with a threshold counter and consequently get more light. Because of the increased signal, the resolution of the differential Čerenkov counter need not be dominated by statistical fluctuations in the number of photoelectrons, but this means that various aberrations of the system now have significant effects on the resolution. Their effect is obtained from Equation (5) to be

$$\left(\frac{\Delta\beta}{\beta}\right)^2 = (\tan\theta\ \Delta\theta)^2 + \left(\frac{\Delta n}{n}\right)^2 \qquad (12)$$

Here $\Delta\theta$ includes contributions from

(a) the finite slit width, which allows a spread of angles $\Delta\theta$ to be detected;

(b) the spread in particle directions; and

(c) aberrations of the spherical mirror due to the particle track illuminating a large fraction of the aperture. Spherical aberration gives $\Delta\theta \sim 1/8(d/f)^3$ and coma gives $\Delta\theta \sim 1/8\ \theta(d/f)^2$. Here f is the focal length of the mirror and the diameter of the region illuminated.

The chromatic aberration, $\Delta n/n$, though negligible in threshold counters, is usually dominant in the differential variety. The velocity resolution of a differential Čerenkov counter may be an order of magnitude better than for a threshold counter of comparable length.

The light passing through the diaphragm is normally detected by a ring of photomultipliers behind the slit. To confirm that there is a ring image centered on the slit requires several tubes in coincidence. The resolution improves with the number, m, in coincidence, but the efficiency falls as

$$\varepsilon = \left(1-e^{-nq}\right)^m \qquad (13)$$

Figure 8 shows a pressure scan for a 10 m Helium filled counter[7] which gives $\Delta\beta/\beta$ of less than 2×10^{-6}.

It is possible to correct for chromatic and spherical aberations and coma by using prismatic optical elements,[8] as indicated in Figure 9. Such counters are referred to as DISC counters and can give improvements in $\Delta\beta/\beta$ by an order of magnitude, i.e., $\Delta\beta/\beta \sim 4\times10^{-7}$. To achieve this value for resolution, uncorrected sources or error, such as the spread in particle directions, must be kept exceedingly small.

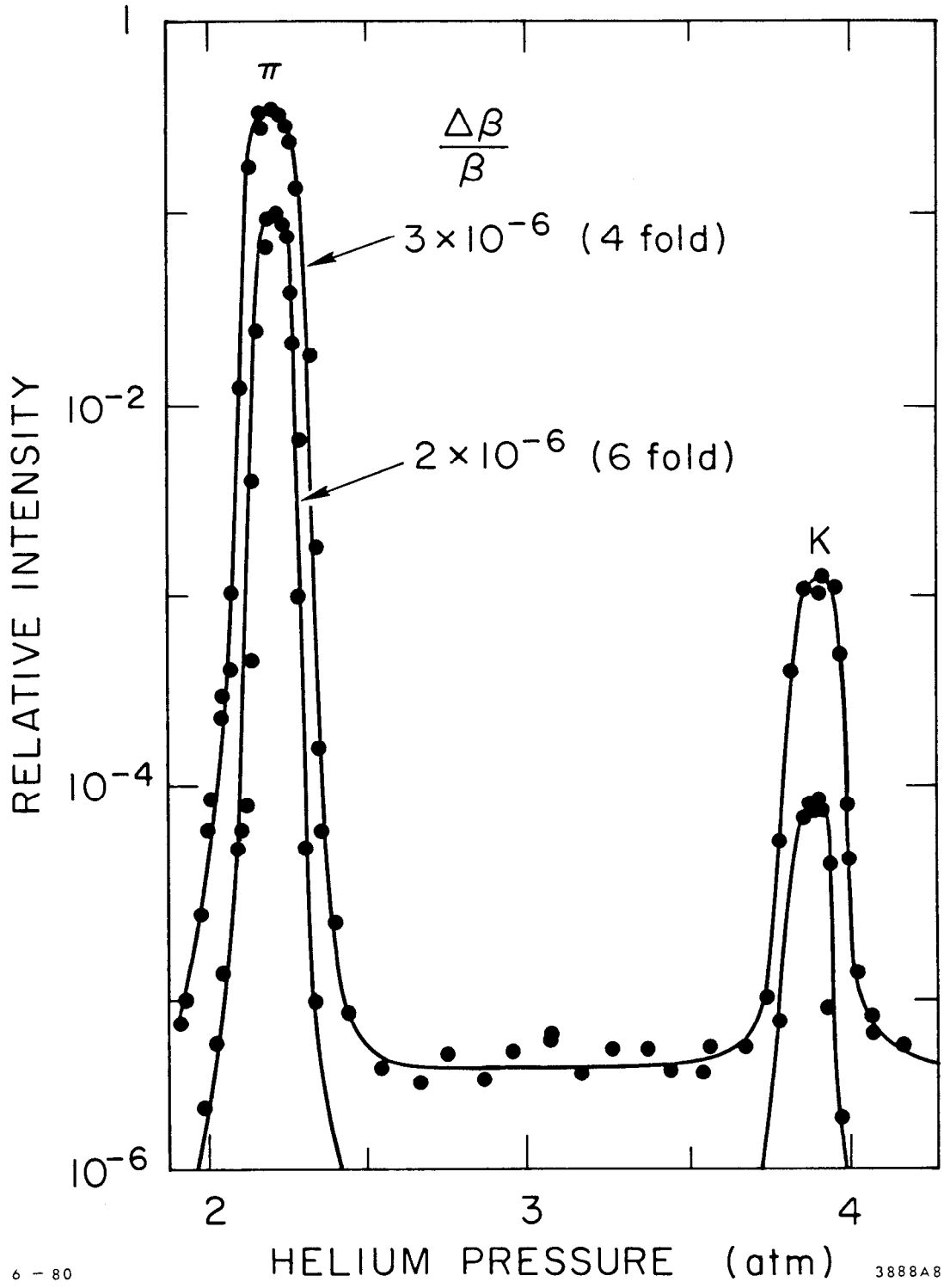

Fig. 8. Pressure scan for a ten meter helium filled differential Čerenkov counter in a 45 GeV/c beam. This shows how rejection of unwanted particles varies with the number of phototubes in coincidence.

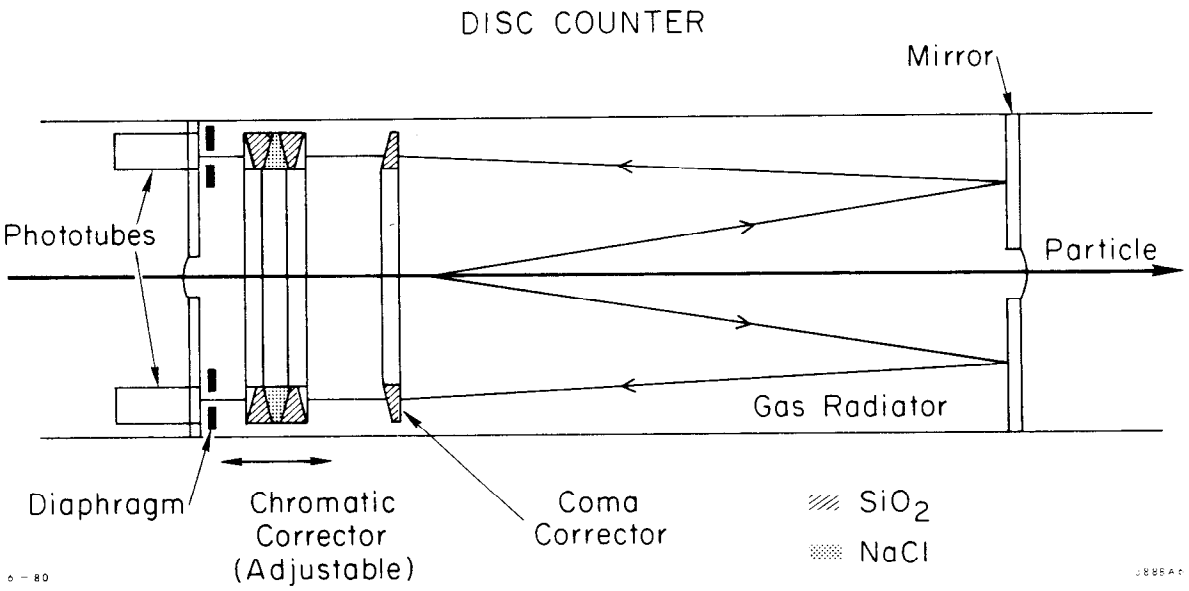

Fig. 9. Gas filled differential Čerenkov counter with optical elements to correct for chromatic abberation and coma.

5. COMPARISON OF DIFFERENTIAL AND THRESHOLD COUNTERS

The differential Čerenkov, operating as it does with larger values of the Čerenkov angle, gives more light for a given length of radiator and hence better $\Delta\beta/\beta$ in general. As shown in Figure 10, this means that the differential counter needed to resolve particles of a given momentum is shorter than the corresponding threshold counter. Other contrasting properties of the two types are listed below.

The differential counter:

- selects specific values of β within a range, $\Delta\beta$,
- imposes severe restrictions on the range of particle directions accepted,
- gives good rejection for unwanted particles.

These properties make the differential Čerenkov most suitable for particle identification in a beam line.

The threshold counter:

- detects all particles with β above threshold,
- can accept a moderate range of directions,
- with segmented optics and detectors it can register several particles simultaneously.
- can operate with the radiator inside a magnet.

The threshold counter is more suited for the detection of particles from an interaction.

6. TRANSITION RADIATION

Equation (2) shows that all Čerenkov counters will have problems at very high momenta, since the error in determining the mass blows up as γ^2. If, instead of determining β, you were able to measure γ

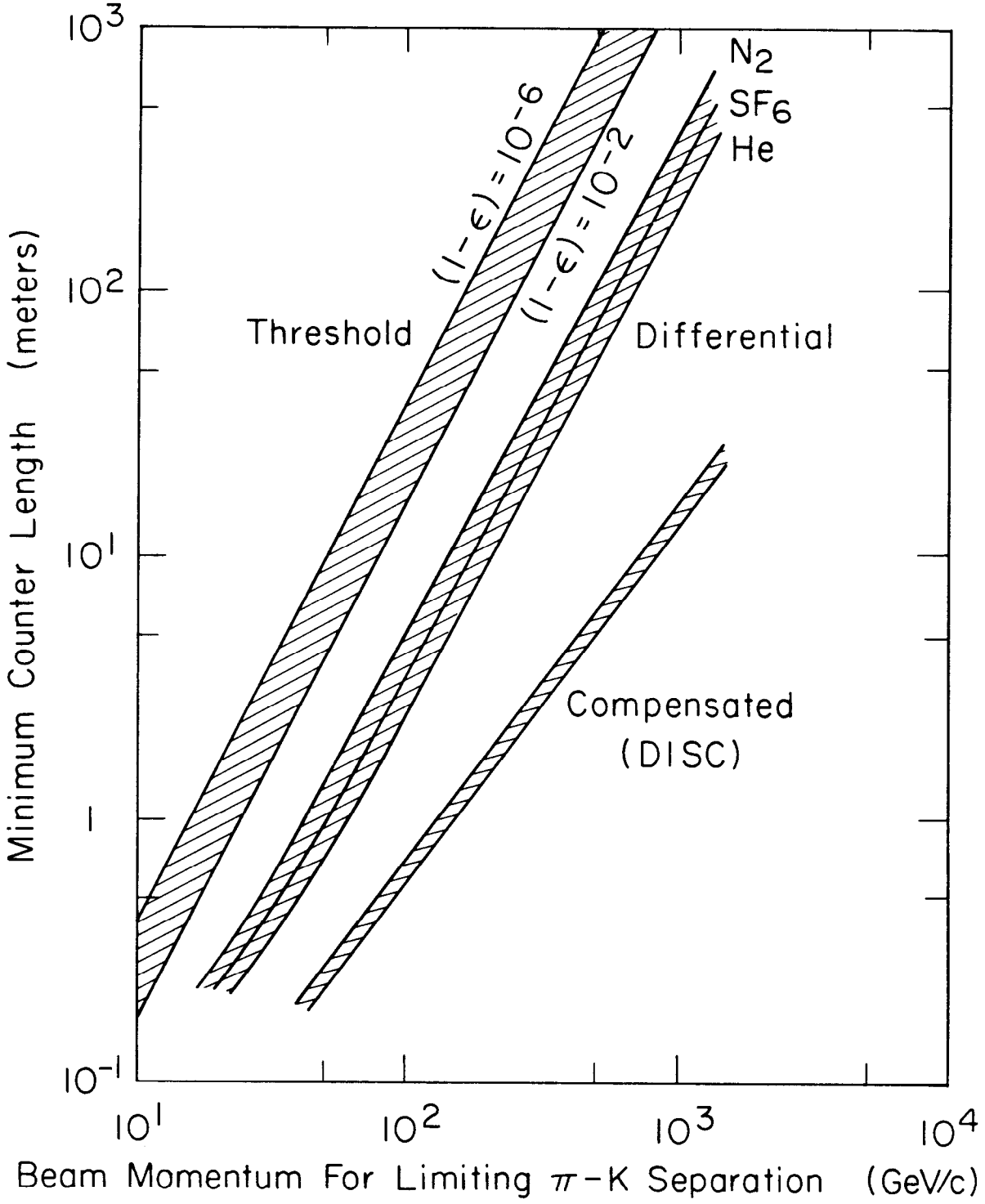

Fig. 10. This plot shows the minimum counter length which permits separation of pions and kaons as a function of momentum, for various counter types. The threshold counter band corresponds to a range of efficiencies ε.

directly, then the appropriate relation would be

$$\left(\frac{\Delta m}{m}\right)^2 = \left(\frac{1}{\beta^2}\frac{\Delta\gamma}{\gamma}\right)^2 + \left(\frac{\Delta p}{p}\right)^2 \qquad (14)$$

If $\Delta p/p$ is small, this gives a mass resolution at high momenta which is proportional to $\Delta\gamma/\gamma$. Ideally you would like a detector whose output is proportional to γ, and this is achieved with transition radiation.[9]

Transition radiation is emitted when a charged particle moves from a medium of refractive index, n_1, to a medium of different index, n_2. This may be thought of as due to the apparent acceleration of the charge. When you look at an object in an optically dense medium, such as a fish in a pond, it appears closer to the surface than it really is. If the fish moves steadily toward the surface it would appear to move more slowly than its actual speed. If, further, it manages by some means to continue to move steadily through the surface, then it would appear to accelerate suddenly. A charged particle moving through such an interface will similarly appear to accelerate and consequently will radiate. Unlike Čerenkov radiation, transition radiation can occur in the x-ray region as there is no requirement that n_1 or n_2 need be greater than one, only that they be different. The radiation can consequently be detected in a proportial chamber, which is an efficient, large area detector.

The energy spectrum for transition radiation between a medium and vacuum is[10]

$$\frac{dI}{d\nu} = \frac{e^2\gamma\omega_p}{\pi c}\left[\left(1 + 2\nu^2\right)\ln\left(1 + \frac{1}{\nu^2}\right) - 2\right] \qquad (15)$$

where ω_p is the plasma frequency for the material and $\nu = \omega/\gamma\omega_p$.

The total energy emitted is then

$$I = \int_0^\infty \frac{dI}{d\nu}\, d\nu = \frac{e^2 \gamma \omega}{3c} \sim \frac{\gamma}{3 \times 137} \hbar\omega_p \qquad (16)$$

This is proportional to γ.

The photons originate from a region around the interface, over which the fields are coherent. This is the formation length D. D is of order $\gamma c/\omega_p$, typically $\gamma \times 10^{-6}$ cm. The angular spread of the transition radiation is very small, being of order $\theta \leq 1/n(\omega)\gamma$. Equation (16) gives the energy spectrum from a single interface, but in practice the radiation is emitted from a stack of foils and each foil has two sides. The spectrum is modified by interference effects, as shown in Figure 11(a), most of the energy being radiated near the frequency of the last maximum. As γ increases, the energy spectrum expands in proportion to γ. For the single interface this should continue indefinitely, but for a foil the output saturates when the energy of the last maximum is $\omega_{max} \sim \ell\omega_p^2/2\pi c$, where ℓ is the foil thickness. This saturation occurs because the increasing output from the single interface is accompanied by a proportional increase in the thickness of the formation length. When the formation length is comparable with the foil thickness it can no longer increase and the output saturates. Figure 11(b) shows the saturation of the γ dependence experimentally.[11]

From Equation (16) it may be seen that the number of photons produced per interface is small, of the order of the fine structure constant, 1/137, each photon having energy of the order $\gamma\hbar\omega_p$. To obtain a reasonable signal you need many interfaces, normally in the form of a stack of thin foils, but x-ray absorption in the material sets a

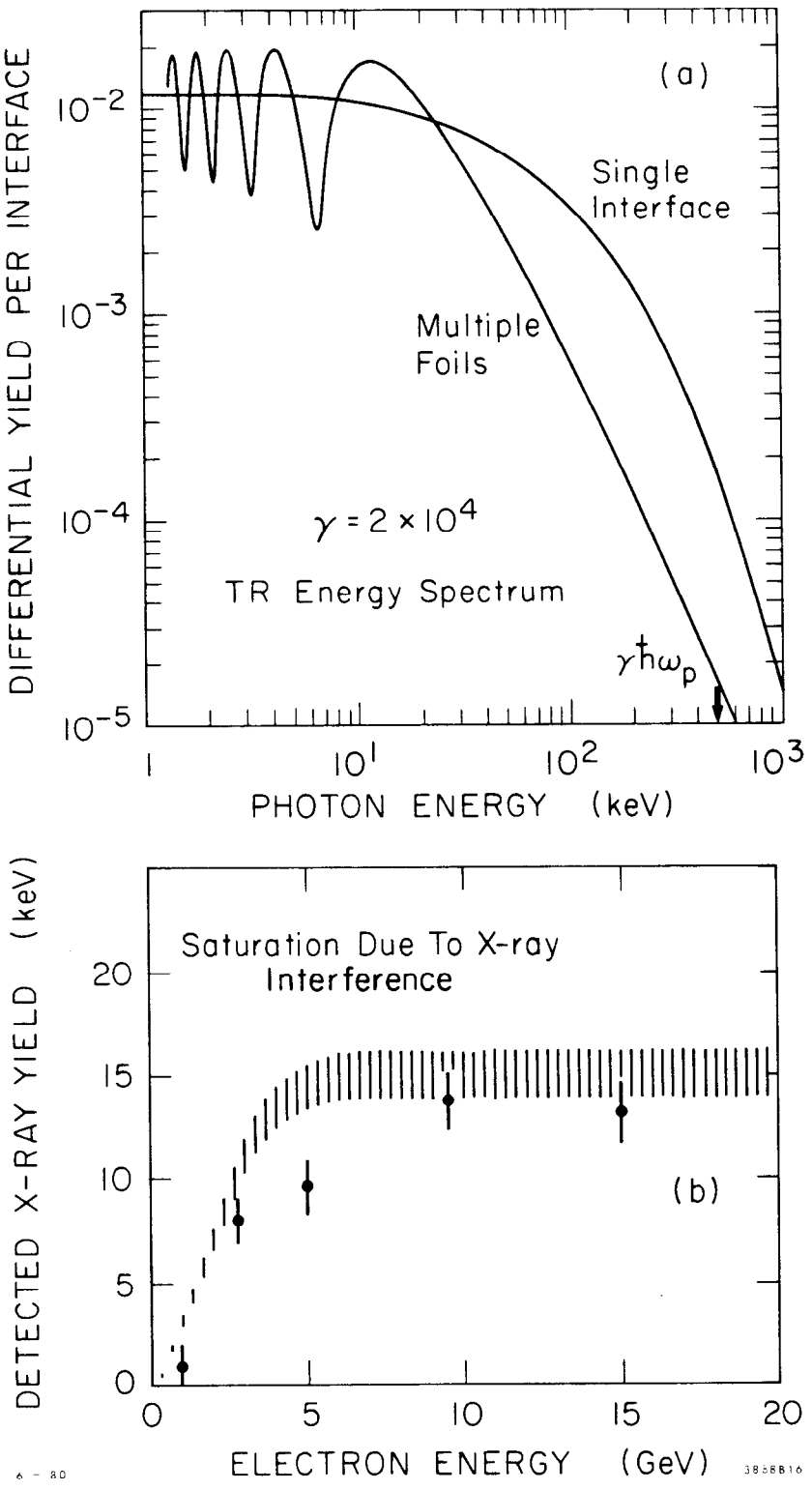

Fig. 11. (a) Transition radiation spectra for radiation from a single interface and from thin foils, showing interference effects, (b) Saturation effect due to foil thickness restricting the formation length.

practical limit on the number. Transition radiation detectors are currently limited by the very low signals obtained. A further problem with transition radiation detection is that the small emission angle means that the T.R. x-rays are not separated from the charged particle in the proportional chamber. You see the T.R. photons plus the ionization loss, dE/dn, for the charged particle.

This superposition of the T.R. photons and the ionizing particle may be avoided by placing a magnet in front of the detector to deflect the particles, as shown in Figure 12(a). In the absence of background due to ionization the x-ray spectrum may be well measured, as in Figure 12(c) which clearly shows interference effects.[12]

Normally the insertion of a deflecting magnet is not practicable and current practice is to optimise the T.R. signal relative to ionization[13] by using Lithium foils of low Z number, to reduce absorption, and thin Xenon filled proportional chambers to detect x-rays with minimum ionization signal. Figure 13 shows the difference in the signal amplitude for pions and electrons of the same momentum.

At present transition radiation detectors are used as electron identifiers,[14] operating with values of γ greater than 10^3 to give a useable signal with acceptable absorption. There is considerable demand for a detector which would identify hadrons at momenta below 100 GeV/c, i.e., with values of γ of the order of 100. The problem here is that the radiation is of lower energy and strongly absorbed. On the other hand, the formation length is small, of the order of a micron, so stacks of very thin foils could be used in principal, though they are difficult to make in practice. Attempts have been made to use polyethylene foams to obtain a large number of interfaces with low mass[15] with

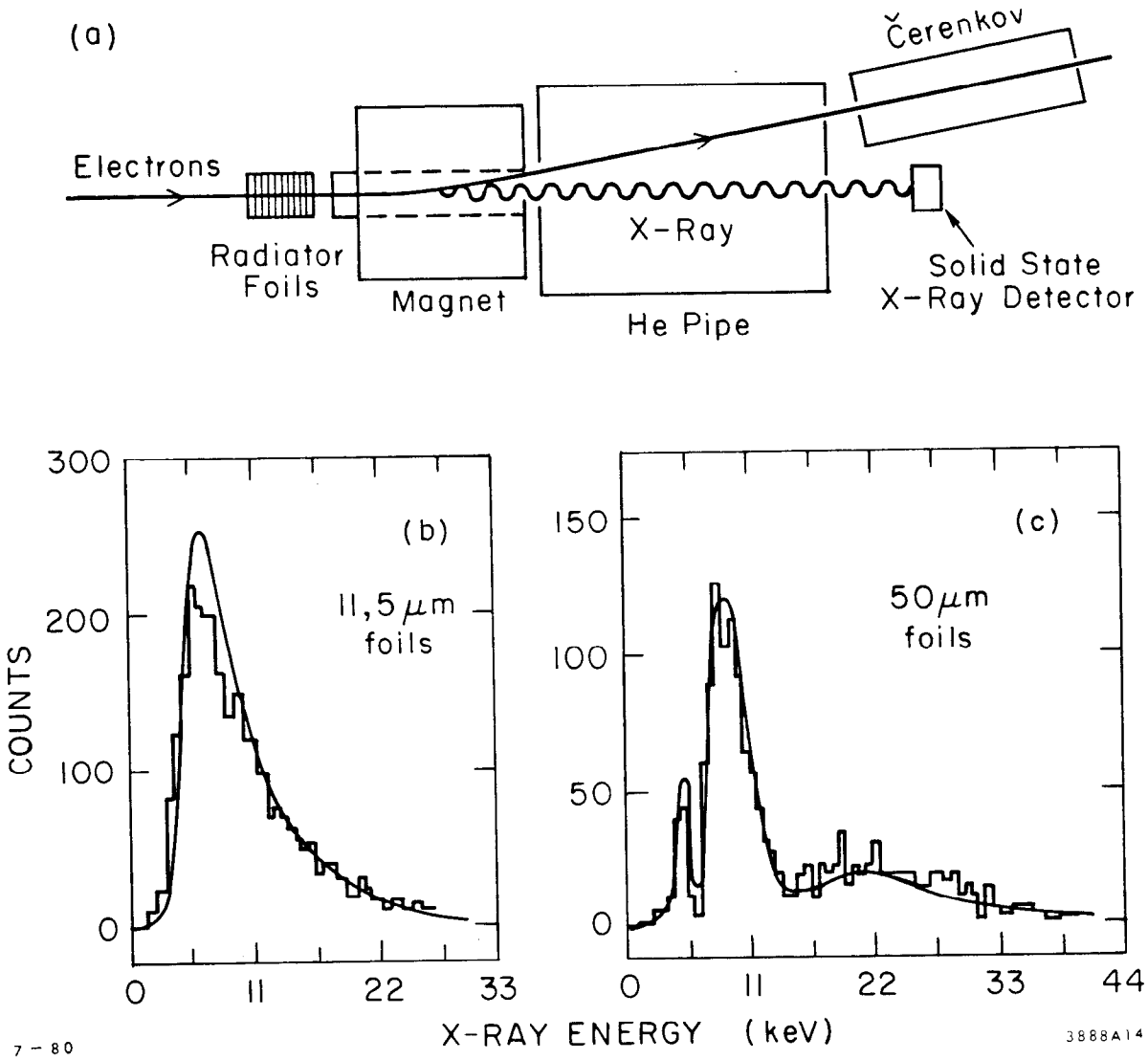

Fig. 12. (a) Detection system with a magnet to sweep particles away from the transition radiation detector; (b,c) show the detailed x-ray energy spectra obtainable.

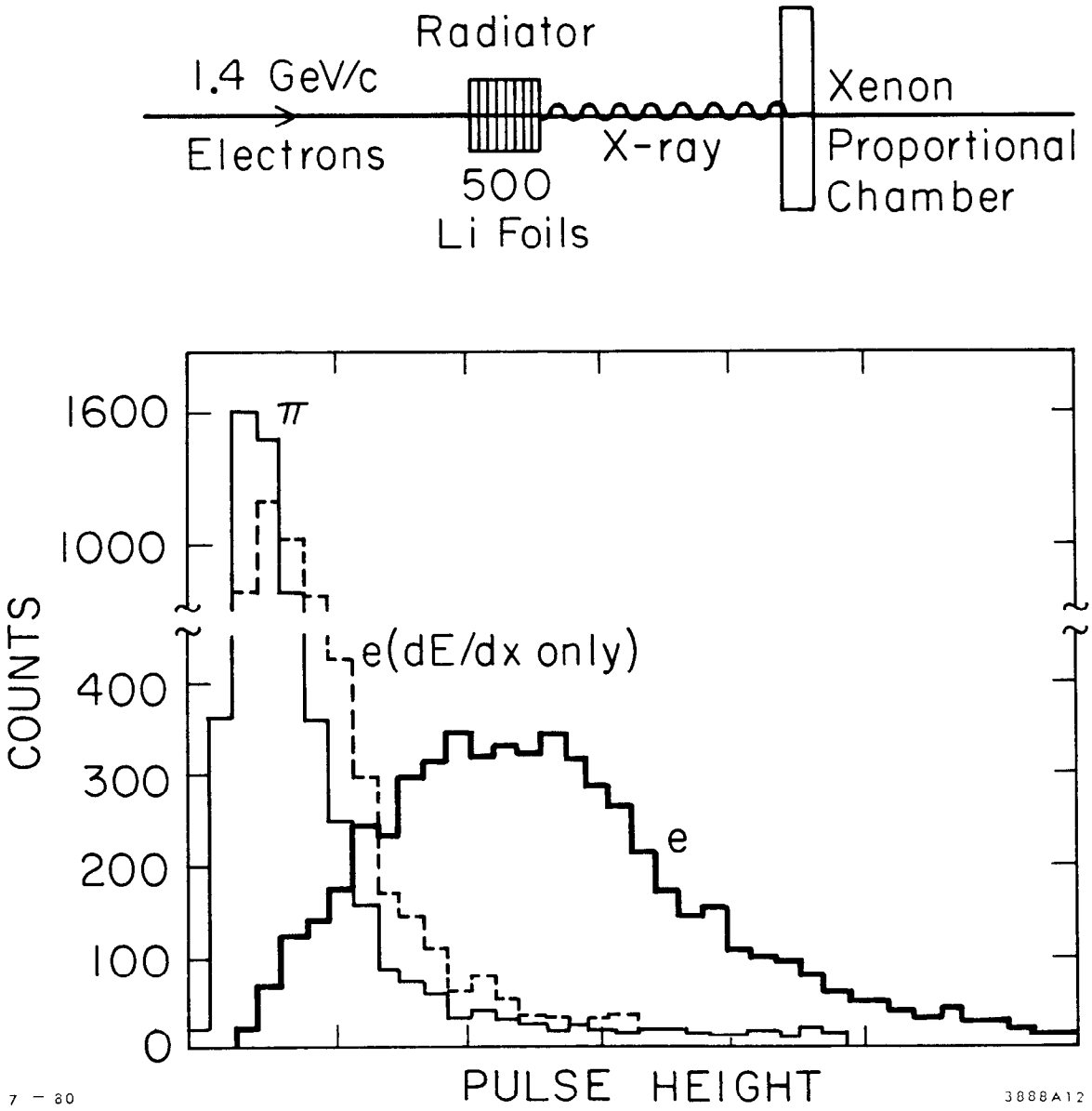

Fig. 13. Practical transition radiation detector with 200 μm Lithium foils; showing a comparison of signals from electrons and pions of 1.4 GeV/c.

some success. Another approach[16] is illustrated in Figure 14, where foils are separated by proportional chambers, so that each gap detects the x-rays produced with minimum absorption. Figure 14(b) shows the separation of protons and pions obtained at p = 200 GeV/c with a total of 18 gaps. With a greater number of gaps and perhaps several thinner foils between each one, it should be possible to obtain hadron separation at 50 GeV/c or lower.

7. RING IMAGING CERENKOV COUNTERS

Transition radiation detectors look good for high momentum particles, but in present high multiplicity events momenta of the order of 10 GeV/c are important and here the Čerenkov counter looks best.

Conventional Čerenkovs have drawbacks when used for identifying scattered particles. The restricted angular acceptance of a differential counter makes it virtually useless. Threshold counters are more practical, but even with molecular construction they are unable to distinguish between multiple particles when they are close together. In neither case does the detector give a measurement of the value of β for a range of possible values. The Čerenkov light contains a great amount of information, it is the detectors which limit it—the objective of the ring imaging Čerenkov is to produce a ring image with a spherical mirror, as in a differential Čerenkov, and then measure the position of each photon detected in this image,[17] as illustrated in Figure 15(a). This requires some form of detector which will give good precision in estimating the coordinates of the detected photons and also have a high efficiency for detecting photons, as the Čerenkov intensity is very low.

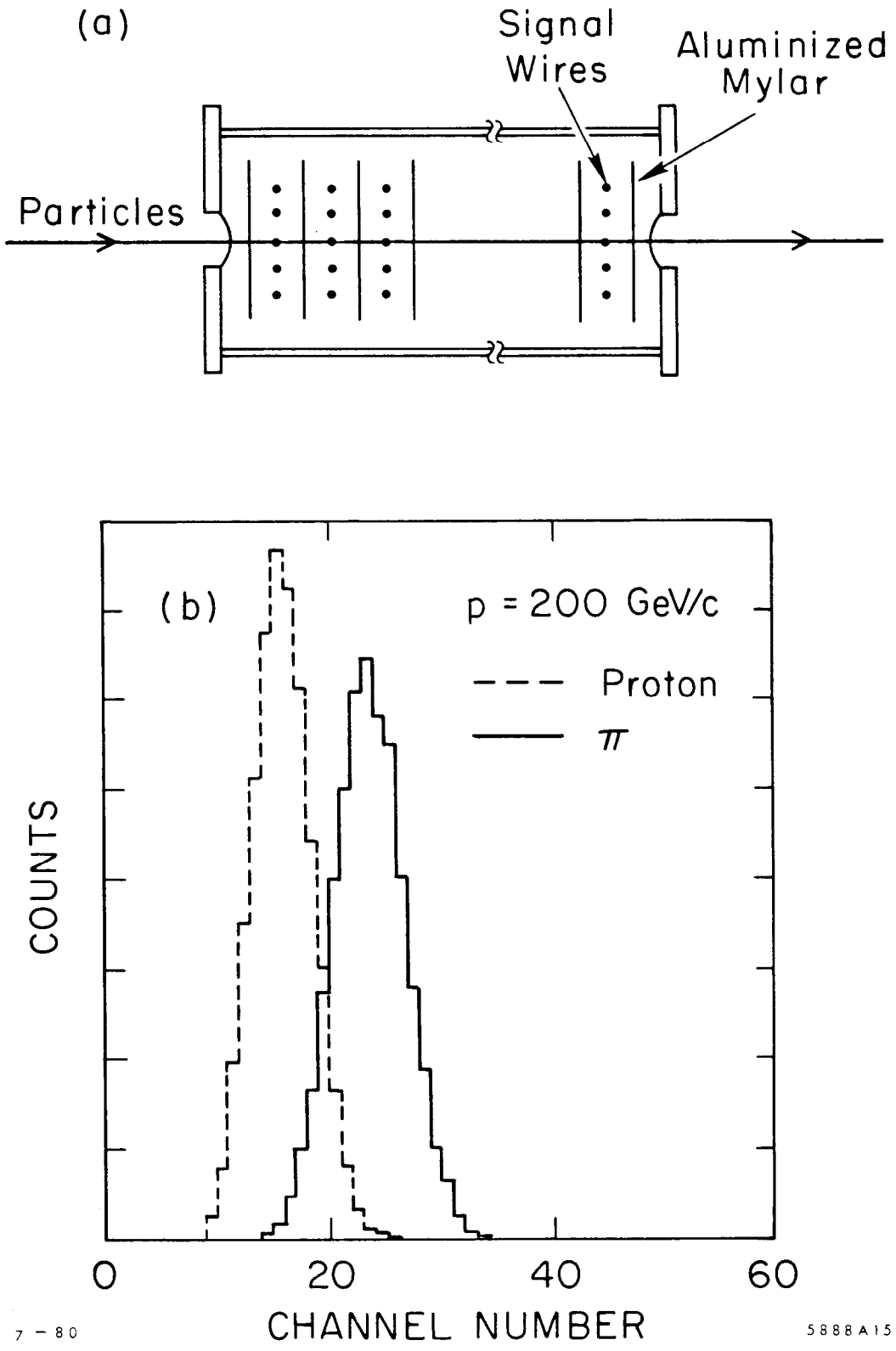

Fig. 14. (a) Prototype detector for hadron separation with 18 proportional chambers, having 4 mm gaps separated by 5 μm foils; (b) shows signals for pions and protons at 200 GeV/c.

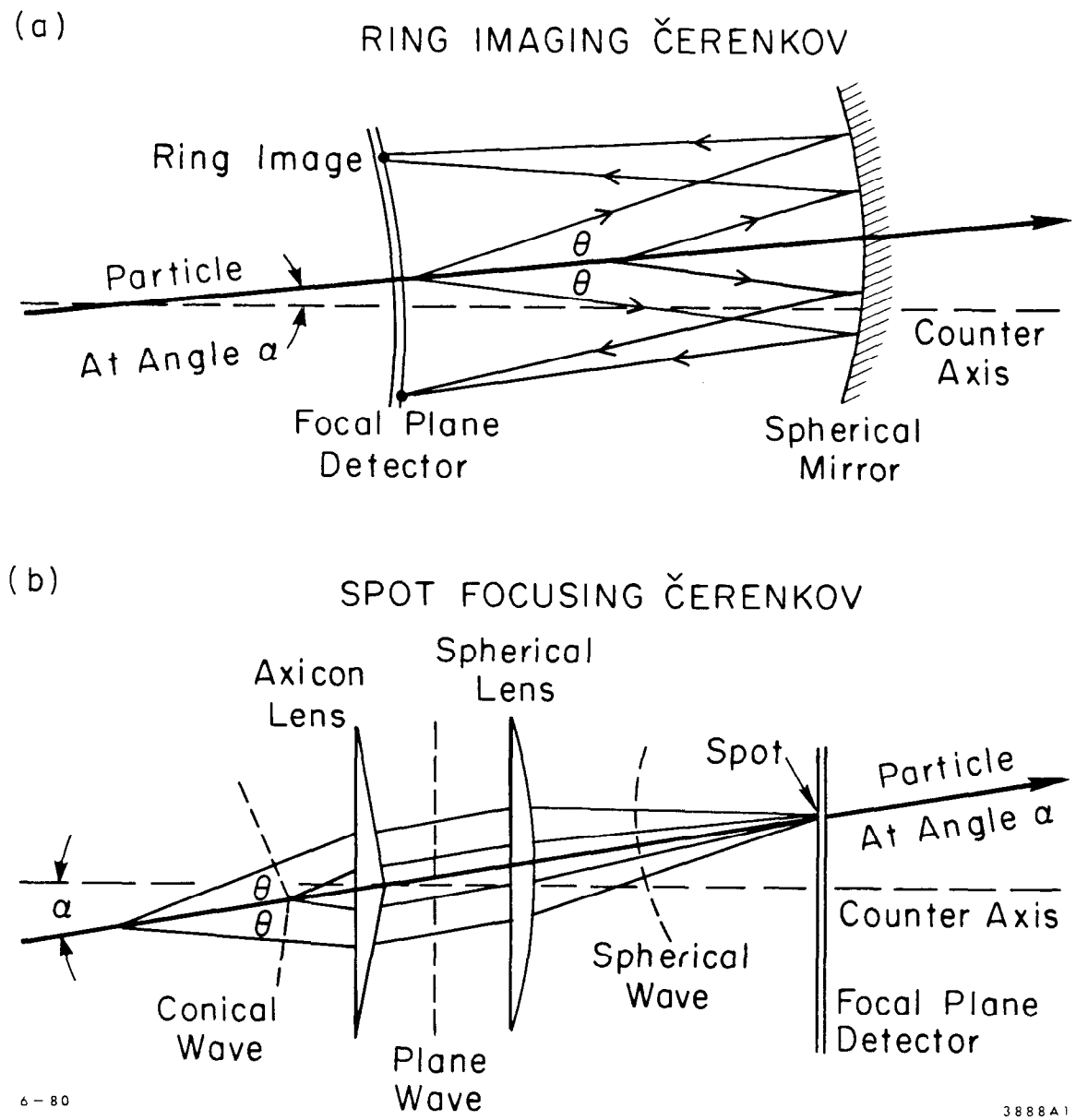

Fig. 15. (a) Principle of ring imaging Čerenkov with detector to measure the position of each photon recorded. (b) Spot focusing detector, which includes an axicon lens to subtract a fixed angle from the Čerenkov cone.

An intermediate concept is the spot focusing detector[18] as shown in Figure 15(b). This in effect subtracts some fixed angle from the Cerenkov cone with the axicon lens, giving a spot image for some preselected β_0. The relative variation of the image size with β around the value β_0 is enhanced, so the detector can be used with a relatively small number of pixels to identify particles with a small range of directions and velocities close to β_0. It is possible to get useable resolution for this device with a matrix of small diameter photubes, but for the "standard" ring imaging concept, without any axicon lens, a high resolution detector with a much larger number of pixels is required.

The full ring imaging Čerenkov would provide a pattern of detected photons as in Figure 16(a), and fit these to appropriate rings for a number of particles (Figure 16(b)).

(a) This gives a measure of β for each particle detected.

(b) The angular range covered can be large if the mirror and detector are large.

(c) It can in principle resolve particles which are close together.

On the other hand there are certain disadvantages. The device is likely to be slow, as the process of fitting rings requires extensive calculation, and it will also be expensive, as it needs an exotic photon detector.

One possibility for detecting the photons is to use an image intensifier[19]—a device with a photocathode similar to a photomultiplier, a microchannel plate to multiply the photoelectrons, and a charge coupled device (CCD) or charge dividing resitive anode[20] to give the coordinates of the photon. Such a system works, and has the advantage of using an established technology, but nevertheless the devices are delicate,

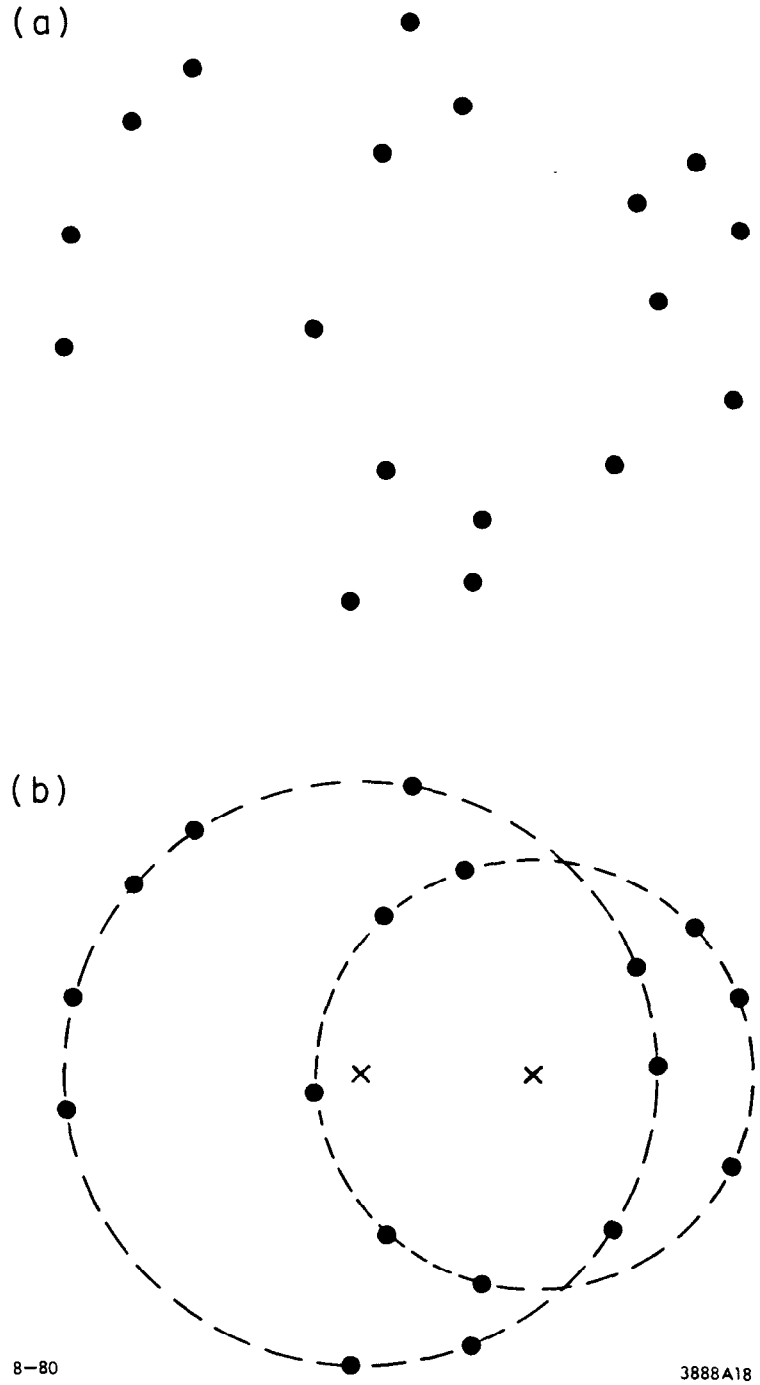

Fig. 16. (a) Possible pattern of detected photons in an imaging Čerenkov; (b) fitted to give Čerenkov ring diameters for two particles.

the quantum efficiency is not as high as for devices using a photoionizing gas, and the detector is small, which requires considerable demagnification of the ring image and limits the angular range of detected particles.

Another approach is the ultraviolet photon detector.[21] The Čerenkov spectrum extends well into the ultraviolet, giving photons with energy of 8 eV and above, which are capable photonionizing some gases with a quantum efficiency which can be as high as 50%. These can be used in a proportional gas chamber to give a large area detector. The range of photon energies which can be detected is limited by the transmission cut-off of available window materials. Figure 17 shows that detection is possible over a useful band. The radiator also must transmit ultraviolet; in practice Nitrogen and a variety of noble gasses have been used.

The photoionizing gas may be included as the low ionization potential gas for a parallel plate avalanche chamber.[22] These chambers can give good high gain output for single photoelectrons, as shown by the single photoelectron pulse height distribution of Figure 18,[23] and the position of the electron avalanche may be detected by a variety of methods. A ring imaging counter can usefully work with a radiator of fairly high refractive index, such as liquid Helium,[24] giving many simultaneous photoelectrons. This means that the readout system must give a unique x,y position for each avalanche. Any system giving a set of x and y values, such as might be obtained with two crossed multiwire chambers, would give rise to many ambiguities. Possible schemes which have been considered are a multiwire proportional chamber,[25] a spark chamber with optical readout,[26] a multigap avalanche chamber with an

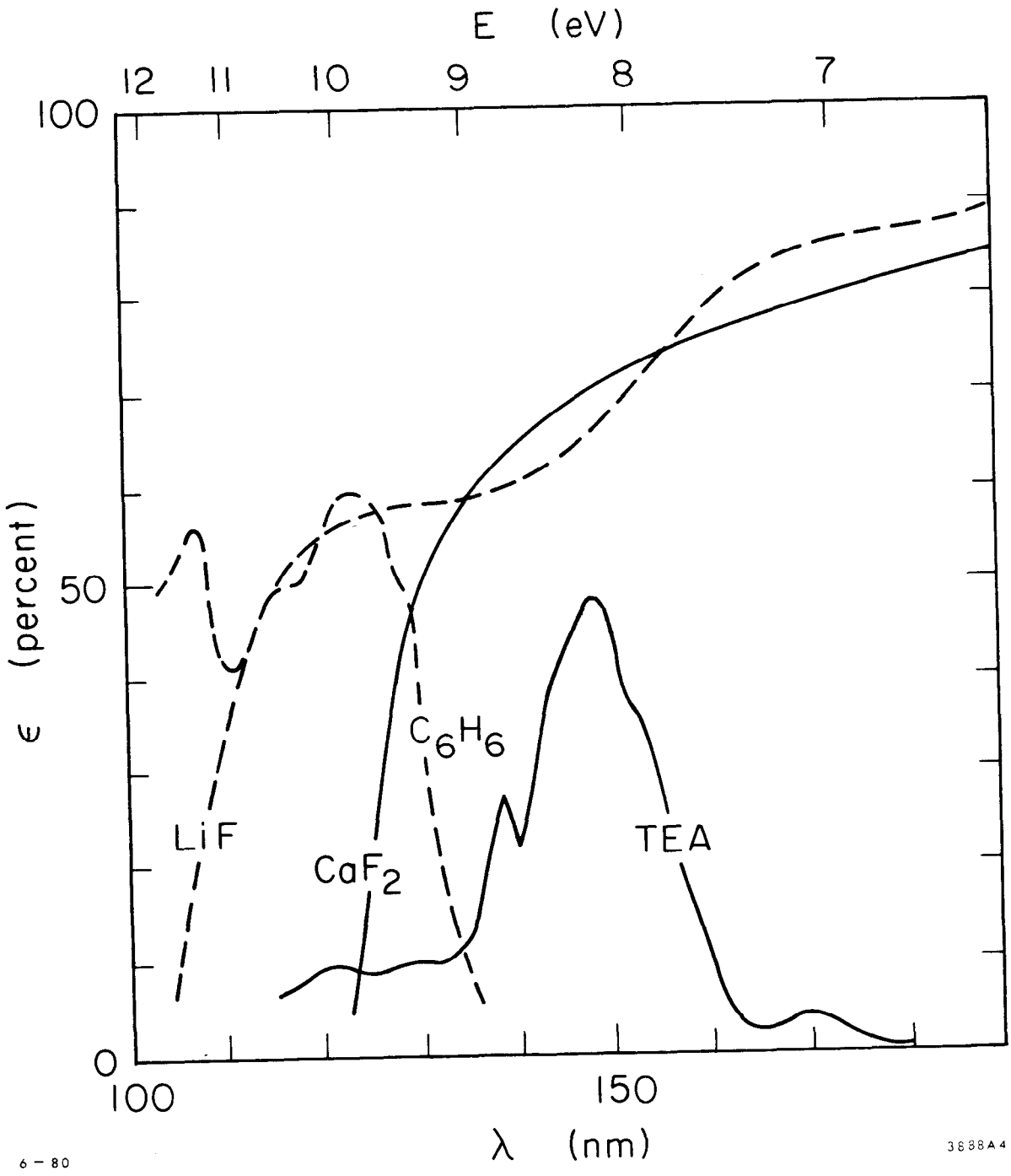

Fig. 17. Variation of photoionizing efficiency and window transmission with photon energy for some materials of interest.

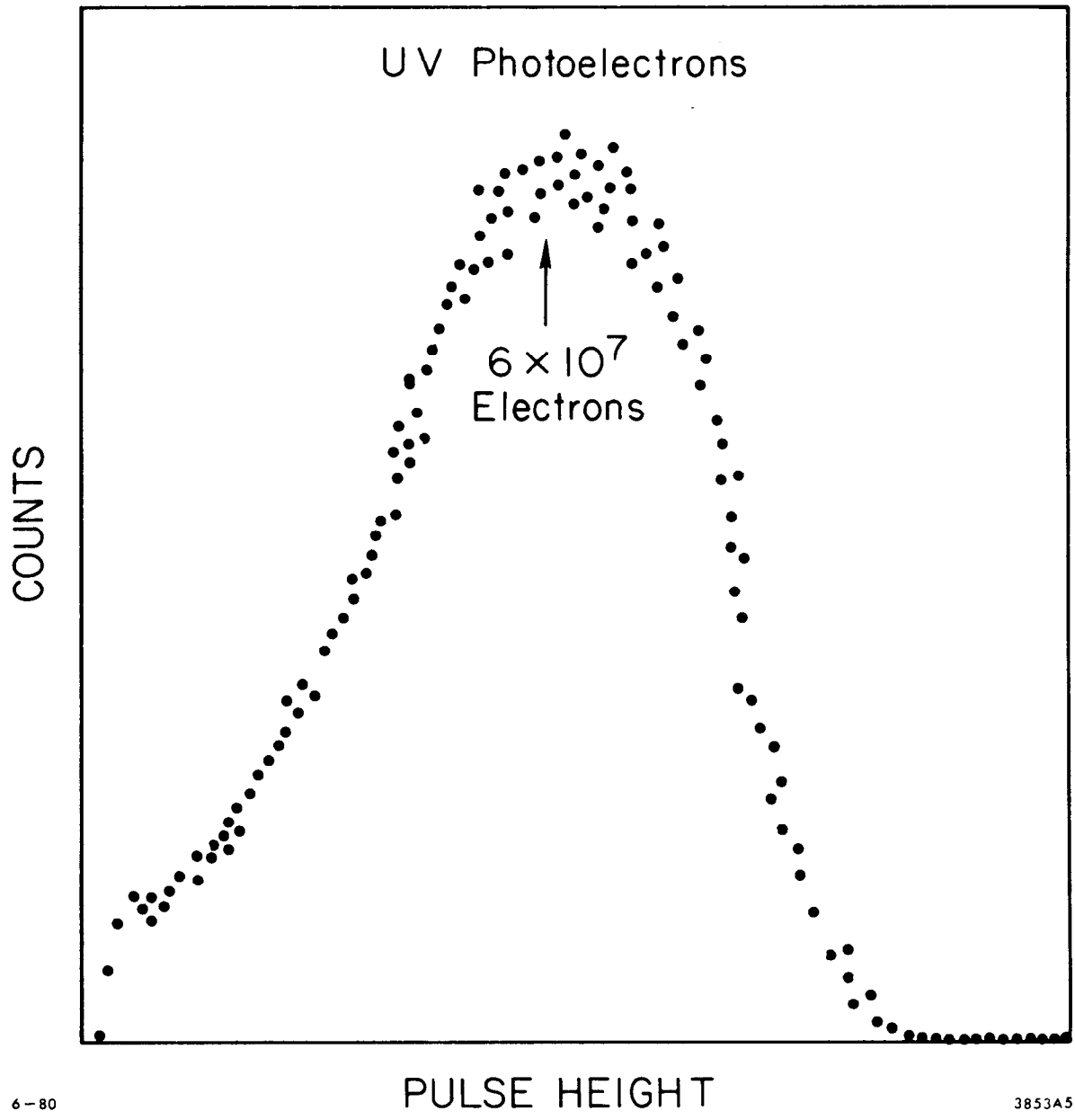

Fig. 18. Pulse height distribution for single photoelectrons amplified in a parallel plate avalanche chamber.

anode divided into small pads,[24] a needle chamber with geiger amplification at the tips[27] and a lateral drift chamber.[28]

Figure 19 is a diagram of a proposed detector. As with the differential Čerenkov, the ring imaging Čerenkov has its resolution limited by aberration, according to Equation (12). For an ultraviolet detecting counter, chromatic dispersion, $\Delta n/n$, is more serious; for photons of 8 eV in Argon it is twice that in the visible region. The uncertainties in the angular term come from factors similar to those for the conventional differential, save that the slit width is replaced by the geometrical error in measuring the position of the photon and the spread in particle directions by the spread in directions for one particle, i.e., the multiple scattering in the radiator. The effect of these terms on the γ resolution (i.e., mass resolution) for kaons of various momenta is plotted in Figure 20, for a radiator one meter long and a precision of 0.6 mm for the photoelectron position. The liquid Helium line corresponds to $\Delta\beta/\beta$ of 5×10^{-4} and the line for the dense gas to $\Delta\beta/\beta$ of 5×10^{-5}.

The ring detector cannot readily be compensated for chromatic and spherical aberration, as with the DISC, but each detected photoelectron gives a separate measurement, so for N photoelectrons the error is reduced by a factor $1/\sqrt{N}$.

The resolution which might be obtained with a ring imaging detector is compared below with values obtained for other types, all counters being five meters long:

$$\text{Threshold} < 10^{-5}\ ,\quad \text{Differential} \sim 3 \times 10^{-6}\ ,\quad \text{DISC} \sim 4 \times 10^{-7}\ ,$$

$$\text{Ring Detector} < 2 \times 10^{-6}\ \text{(estimated)}\ .$$

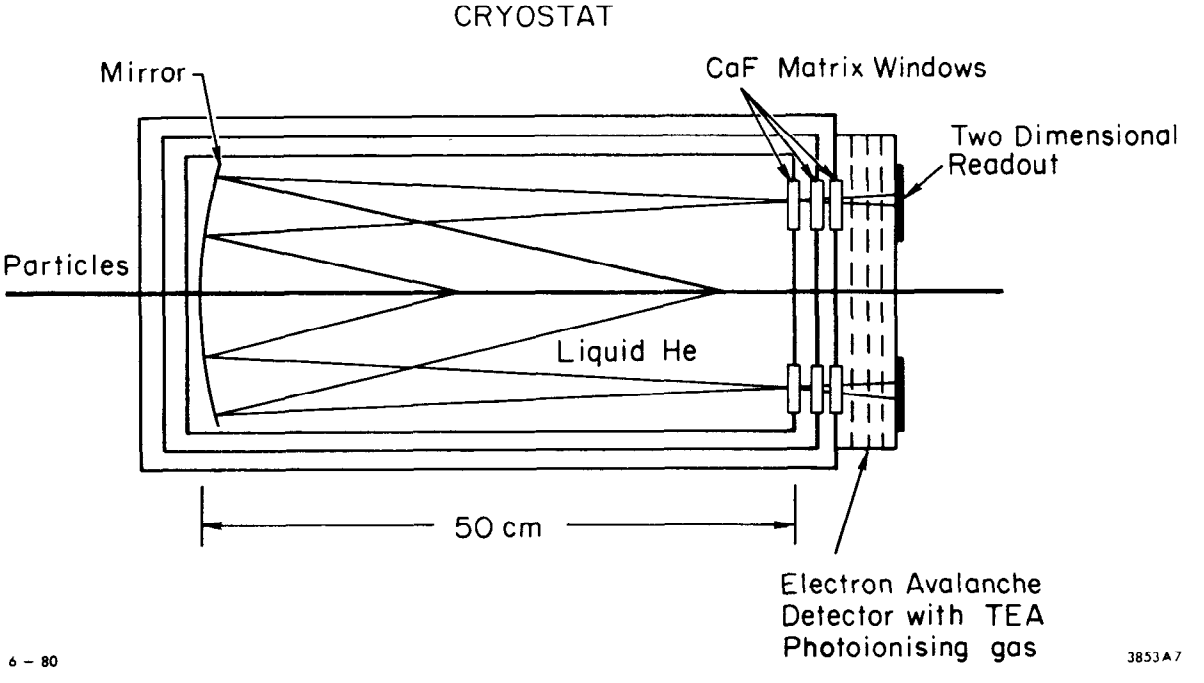

Fig. 19. A proposed prototype detector.

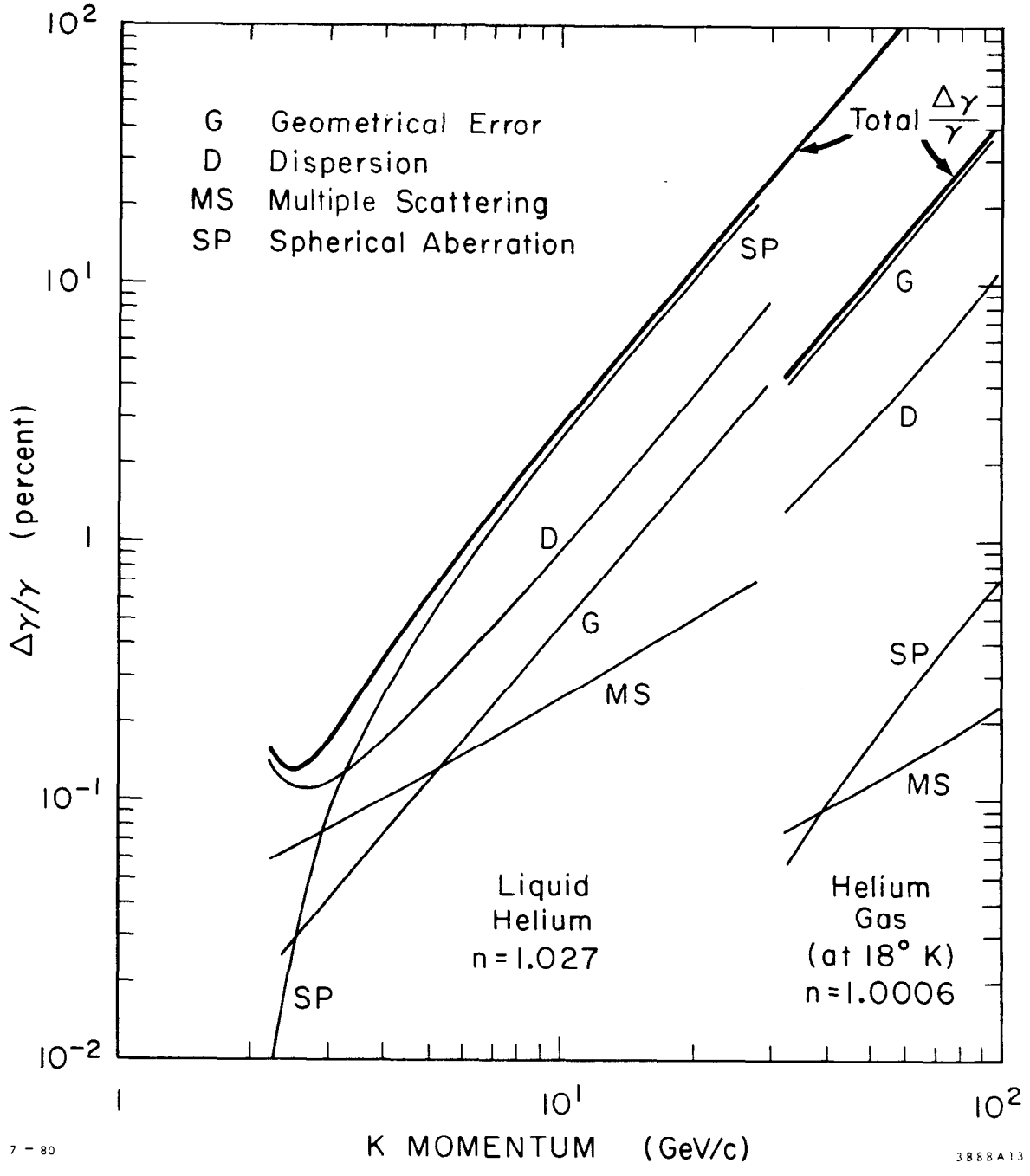

Fig. 20. Comparison of the effect of different sources of aberation on the resolution of an ultraviolet ring imaging Čerenkov counter one meter long, with a photon detector of 0.6 mm resolution.

The value estimated for the ring imaging Čerenkov assumes a low refractive index, with a consequent high β threshold. In practice it would normally be operated with a lower threshold, to give a wide coverage of β, and the resolution would be worse.

The resolution of the imagining Čerenkov is much poorer than that attainable with a compensated differential (DISC). Its advantages are in its wide angular coverage and ability simultaneously to measure the values of β for several particles of different velocities.

8. CONCLUSIONS

The Čerenkov counter has a role as a particle identifier for velocities which are too high for Time-of-Flight to be used, and too low for transition radiation detectors to give a useable signal. In beam lines the compensated differential counter is capable of giving the best resolution, but at high momenta the restriction on the spread of particle directions gives unacceptable limits on the beam acceptance. The transition radiation detectors being developed to identify hadrons at relatively low momentum do not have this restriction and might be used instead.

For particles produced in an interaction, the ring imaging type of Čerenkov should give the best coverage for multiparticle events, but a threshold counter is much simpler, cheaper and faster where it can give adequate separation. Again at high values of γ the resolution of Čerenkov counters will fail and some form of transition radiation detector will be necessary.

REFERENCES

1. J. D. Jackson, Classical Electrodynamics, Second Edition, John Wiley (N. Y.) 1975, p. 638.

2. J. Litt and R. Meunier, Ann. Rev. of Nucl. Sci 23, 1 (1973).

3. M. Cantin et al., Nucl. Instrum. Methods 118, 177 (1974); P. J. Carlson, K. E. Johansson and J. Norrby, IEEE Trans. on Nucl. Sci. NS-27, 96 (1980).

4. S. P. Denisov et al., Nucl. Instrum. Methods 85, 101 (1970).

5. P. Baillon et al., Nucl. Instrum. Methods 126, 319 (1975); P. J. Carlson, Nucl. Instrum. Methods 158, 403 (1979).

6. B. Alper et al., Phys. Lett. B94, 422 (1980).

7. S. P. Denisov et al., Nucl. Instrum. Methods 92, 77 (1971).

8. R. Meuniér, NAL Summer Study Rep SS/170, 85 (1970); C. Bovet, S. Milner, A. Placci, IEEE Trans. Nucl. Sci. NS-25, 572 (1978).

9. Proceedings of International Symposium on Transition Radiation of High Energy Particles, Yerevan, 1977; S. Iwata, report DPNU-31-79 (1979).

10. J. D. Jackson, op. cit., p. 691.

11. M. L. Cherry, G. Hartman, D. Müller and T. A. Prince, Phys. Rev. D10, 10 (1974).

12. C. W. Fabjan and W. Struczinski, Phys. Lett. 57B, 483 (1975).

13. J. Fischer et al., Nucl. Instrum. Methods 127, 525 (1975).

14. J. Cobb et al., Nucl. Instrum. Methods 140, 413 (1977).

15. C. W. Fabjan, Proceedings of International Symposium on Transition Radiation of High Energy Particles, Yerevan, 1977, p. 256.

16. A. G. Oganessian et al., Nucl. Instrum. Methods 145, 251 (1977).

17. A. Roberts, Rev. Sci. Instrum. 31, 579 (1960).

18. M. Benot, J. M. Howie, J. Litt and R. Meuniér, Nucl. Instrum. Methods 111, 397 (1973); M. Benot, J. C. Bertrand, A. Maurer and R. Meuniér CERN report CERN-EP/79-51.

19. B. Robinson, Report UPR-76E (1980), submitted to the Conference on Experimentation at LEP, Uppsala, 1980.

20. J. L. Alberi and V. Radeka, IEEE Trans. on Nucl. Sci., NS-23, 251 (1976).
J. W. Stümpel, P. W. Sanford, and H. F. Goddard, Journal of Physics E, 397 (1973).

21. J. Seguinot and T. Ypsilantis, Nucl. Instrum. Methods 142, 377 (1977).

22. G. Charpak and F. Sauli, Phys. Letters 78B, 523 (1978);
A. Breskin et al., Nucl. Instrum. Methods 161, 19 (1979).

23. R. S. Gilmore, D.W.G.S. Leith, S. H. Williams, paper submitted to IEEE 1980 Nuclear Science Symposium.

24. S. H. Williams, D.W.G.S. Leith, M. Poppe and T. Ypsilantis, IEEE Trans. on Nucl. Sci. NS-27, 91 (1980).

25. J. Seguinot, J. Tocqueville and T. Ypsilantis, Nucl. Instrum. Methods 173, 283 (1980).

26. G. Charpak, S. Majewski, G. Melchart, F. Sauli and T. Ypsilantis, Nucl. Instrum. Methods 164, 419 (1979).

27. G. Comby and P. Mangeot, IEEE Trans. on Nucl. Sci. NS-27, 111 (1980).

28. T. Ekelöf, J. Seguinot, J. Tocqueville and T. Ypsilantis, paper submitted to the International Conference on Experimentation at LEP, Uppsala, 1980.